RECENT B PHYSICS RESULTS FROM CLEO

Eckhard von Toerne

Kansas State University,
Manhattan, KS 66506-2601
evt@phys.ksu.edu

Representing the CLEO Collaboration

ABSTRACT

The CLEO detector is located at the CESR $\mathrm{e^+e^-}$ collider in Ithaca, NY. CLEO's wide range of experimental measurements in b-hadron decays is represented by improved measurements of $\mathrm{V_{cb}}$ and $\mathrm{V_{ub}}$, rare B decays, and $b\overline{b}$ spectroscopy. New experimental results in exclusive hadronic transitions will aid theorists in developing a theory of hadronic B decays. Such a theory will have consequences for the extraction of angles of the unitarity triangle, especially γ. Recently, the CLEO collaboration has shifted its focus towards precision measurements at lower energies. Based on the new $\Upsilon(3S)$ data, we present the observation of a new bound $b\overline{b}$ state. An outlook on the planned running at τ/charm-energies (CLEO-c) is given and the implications for b-physics are discussed.

Invited talk at
"Secrets of the B Meson", SSI 2002 Topical Conference,
Stanford, CA, August 2002

1 Introduction

The advent of high-luminosity B factories and the discovery of time-dependent CP asymmetries in the B-system[1,2] has transformed the whole field of B physics. Precision tests of the standard model open up a window for the discovery of new physics in B decays. This will require a thorough understanding of time-dependent phenomena like mixing, and also **time-independent** phenomena like branching fractions and particle spectra. Effects like final state interactions, re-scattering and interference between dominant and suppressed decay amplitudes have to be understood. This makes it necessary to study extensively numerous rare and hadronic B decays to gain full understanding of the dynamics.[3,4,5]

The CLEO collaboration has accumulated a large data set of 16 fb^{-1} at the $\Upsilon(4S)$ resonance with the CLEO-II, II.5 and III detector configurations. Almost 50% of data set were recorded with CLEO-III in a single year. This impressive achievement proved to be insufficient to match the luminosity records of the B-factories Babar and Belle. CLEO returned to the Υ resonances below $B\overline{B}$ threshold ($\Upsilon(1S)$,$\Upsilon(2S)$,$\Upsilon(3S)$) to collect data samples above or close to the total world data sets. Most results presented here are based on the CLEO II and II.5 data. The integrated luminosity of this subsample is 9.1 fb^{-1}, collected on the $\Upsilon(4S)$ resonance and 4.3 fb^{-1} $\sim$60 MeV below the resonance to study the continuum background from $\mathrm{e^+e^-} \to \mathrm{q\overline{q}}$. The importance of the *large* off-resonance sample lies in the background subtraction neccessary in inclusive measurements such as $b\to s\gamma$ or the extraction of $\mathrm{V_{ub}}$ in the lepton energy endpoint region.

Detector	Resonance fb^{-1}	Continuum fb^{-1}	$B\overline{B}$ (10^6)
CLEO II	3.1	1.6	3.3
CLEO II.V	6.0	2.8	6.4
Subtotal	9.1	4.4	9.7
CLEO III ($\Upsilon(4S)$)	6.9	2.3	7.4
Total ($\Upsilon(4S)$)	16.0	6.7	17.1

Table 1. *Integrated luminosities (on- and off-resonance) and the number of $B\overline{B}$ pairs.*

The CLEO II.5 and III detectors are shown in Figure 1. The outer detector parts, the CsI calorimeter, superconducting coil, magnet iron and muon chambers are common to

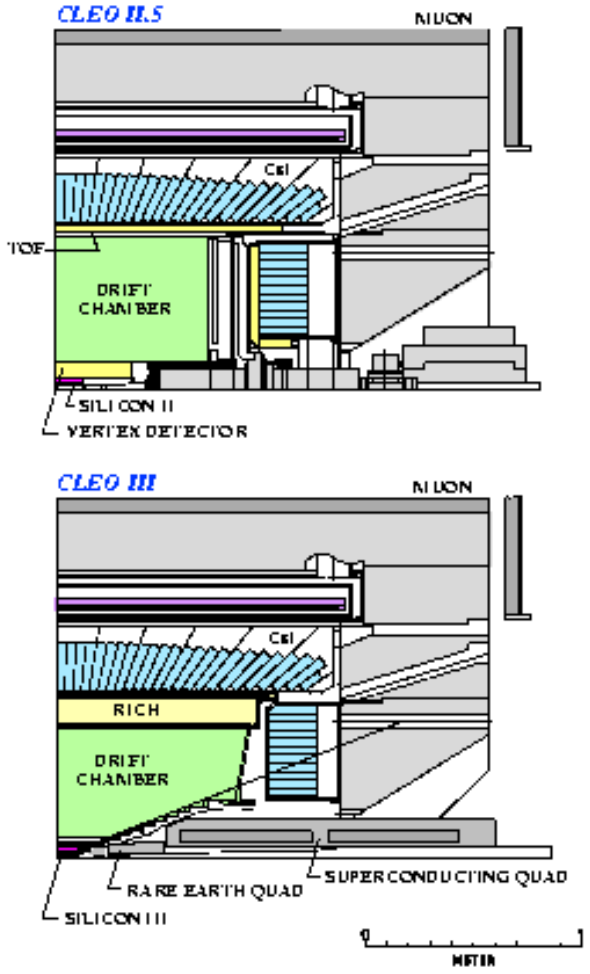

Fig. 1. *Quarter sections of the CLEO-II.5 and CLEO-III detector configurations.*

all three detector configurations. In the CLEO III upgrade, the CLEO II.5 silicon vertex detector, drift chamber and time-of-flight counters were replaced by a new silicon vertex detector, drift chamber, and a new Ring Imaging Cherenkov detector. Table 1 shows the integrated luminosities obtained with each detector configuration.

The kinematics of the $\Upsilon(4S)$ decay, in which two B mesons with equal masses are produced, allow us to define two sensitive variables: the beam-constrained mass $\mathrm{M_B} = \sqrt{\mathrm{E^2_{beam}} - \mathrm{P^2_B}}$ and the energy difference $\Delta\mathrm{E} = \mathrm{E_B} - \mathrm{E_{beam}}$, where $\mathrm{E_B}$ and $\mathrm{P_B}$ are the measured energy and momentum of the B candidate and $\mathrm{E_{beam}}$ is the beam energy.

The CLEO collaboration and CESR plan to operate at center-of-mass energies in the τ/charm region.[6] This will expand the scope of our on-going charm physics program and will allow precision tests of perturbative QCD and lattice QCD predictions. I will later explain the impact that these results, taken at lower energy, will have on B physics.

2 Semi-Leptonic B decays

The partial semileptonic decay width $\Gamma^{\rm c}_{\rm SL} = \Gamma(\overline{\rm B}\to {\rm X_c}\ell\overline{\nu})$ is proportional to $|{\rm V_{cb}}|^2$, $\Gamma^{\rm c}_{\rm SL} = \gamma_{\rm c}|{\rm V_{cb}}|^2$, with the proportional factor γ_c being dependent on perturbative and non-perturbative parameters. The precision of the determination of $|{\rm V_{cb}}|$ is mainly limited by uncertainties on the parameters entering the expression for γ_c. Semi-leptonic rates and spectra can be expanded in a power series. To order $1/M_B^3$ the decay width is[7]

$$\Gamma^c_{SL} = \frac{G_F^2|{\rm V_{cb}}|^2 M_B^5}{192\pi^3}(G_0 + 1/M_B G_1(\overline{\Lambda}) + 1/M_B^2 G_2(\overline{\Lambda},\lambda_1,\lambda_2) + 1/M_B^3 G_3(\overline{\Lambda},\lambda_1,\lambda_2|_{\rho_1,\rho_2,\tau_1,\tau_2,\tau_3,\tau_4})),$$

with known functions $G_{0,1,2,3}$ and three main perturbative parameters $\overline{\Lambda}, \lambda_1, \lambda_2$, which are accessible through experimental measurements. The parameter λ_1 is related to the average kinetic energy of the b-quark inside the B meson. The parameter λ_2 is the expectation value of the leading operator that breaks the heavy quark symmetry and can be determined from the $B^* - B$ mass splitting. $\overline{\Lambda}$ is related to the b-quark pole mass m_b. The dependence on the remaining parameters ρ_i, τ_j is expected to be relatively weak.

Moments of lepton spectra in semileptonic B decays. CLEO has pioneered measurements of moments of the hadronic mass spectrum in $B\to X_c\ell\nu$ decays.[8] Our measurement together with the measurement of moments in $b\to s\gamma$[9] allowed us to extract the perturbative parameters λ_1 and $\overline{\Lambda}$. A new CLEO result[10] involving moments constitutes an important cross check to our previous analysis. The lepton energy spectrum has been analyzed following a suggestion from M. Gremm, A. Kapustin, Z. Ligeti and M. B. Wise.[11] The two ratios extracted from the data are

$$R_0 = \frac{\int_{1.7}(d\Gamma_{sl}/dE_\ell)dE_\ell}{\int_{1.5}(d\Gamma_{sl}/dE_\ell)dE_\ell}$$

$$R_1 = \frac{\int_{1.5}(E_\ell d\Gamma_{sl}/dE_\ell)dE_\ell}{\int_{1.5}(d\Gamma_{sl}/dE_\ell)dE_\ell}$$

The lepton spectrum was truncated to lepton momenta above 1.5 GeV in order to reduce the systematic uncertainty due to secondary leptons from the cascade decays $b\to c\to s$. The spectra for electrons and muons yield consistent results (Fig. 2, left). The combined electron and muon result is

$$\overline{\Lambda} = (0.39 \pm 0.03 \pm 0.06 \pm 0.12)\, GeV \quad \lambda_1 = (-0.25 \pm 0.02 \pm 0.05 \pm 0.14)\, GeV^2,$$

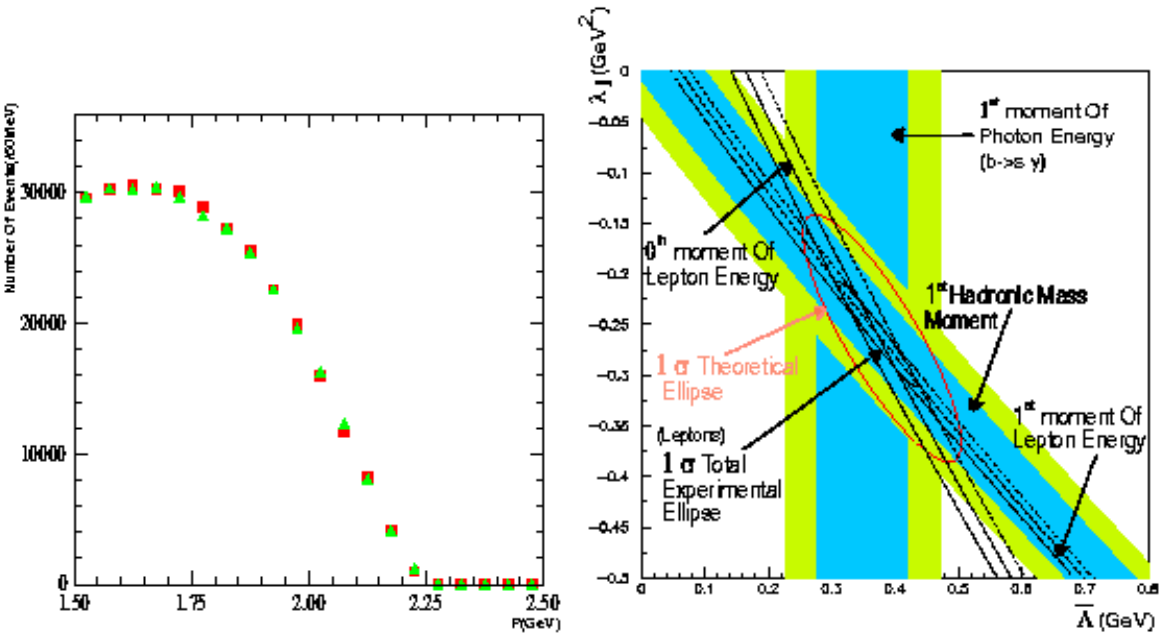

Fig. 2. **(left)** *Electron (green triangles) and Muon spectra (red squares) above 1.5 GeV, evaluated in the B-meson rest frame.* **(right)** *Constraints from the $\overline{B}\to X_c\ell\overline{\nu}$ hadronic mass moments and $b\to s\gamma$ compared with the combined electron and muon R_0 and R_1 results.*

where the errors are statistical, systematic and theory error, respectively. The fact that the parameters extracted from lepton momentum spectra and hadronic mass moments yield consistent results (as shown in Fig. 2, right), represents a valuable cross check of the theory and its underlying assumptions.

$\mathrm{V_{cb}}$ **from exclusive decays** The decay $B\to D^*\ell\nu$ is a prime candidate for the extraction of $\mathrm{V_{cb}}$ from exclusive decays. CLEO analyzes[12] D^{*0} and D^{*+} modes and obtains $\mathcal{B}(\overline{\mathrm{B}}^0\to D^{*+}\ell^-\overline{\nu}) = (6.09 \pm 0.19 \pm 0.40) \times 10^{-2}$ and $\mathcal{B}(B^-\to D^{*0}\ell^-\overline{\nu}) = (6.50 \pm 0.20 \pm 0.43) \times 10^{-2}$. We determine the yield as a function of $\mathcal{W}$, the boost of the D^* in the B rest frame. The decay rate $d\Gamma/d\mathcal{W}$ extrapolated to the kinematic endpoint ($\mathcal{W} = 0$) can be calculated in Heavy Quark Effective Theory and is proportional to $|\mathrm{V_{cb}}|^2$. The shape of $d\Gamma/d\mathcal{W}$ can be expressed with only one free parameter ρ, which is approximately the slope of the distribution in Fig. 3 (c). The two B decay modes give results that are consistent with each other. The combined result is

$$|\mathrm{V_{cb}}| = 0.0469 \pm 0.0014(stat) \pm 0.0020(syst) \pm 0.0018(theor.),$$

where the systematic error is dominated by the uncertainty on the form factor calculation from lattice QCD, $\mathcal{F}(1) = 0.92 \pm 0.03$.

CLEO is the only experiment so far that has measured both the D^{*+} and the D^{*0} decay modes. Our combined measurement is slightly higher than LEP and the B factory measurements, employing the same method for D^{*+} only. The consistency of our result with these measurements is at the 5% level[7] (Fig. 3, d).

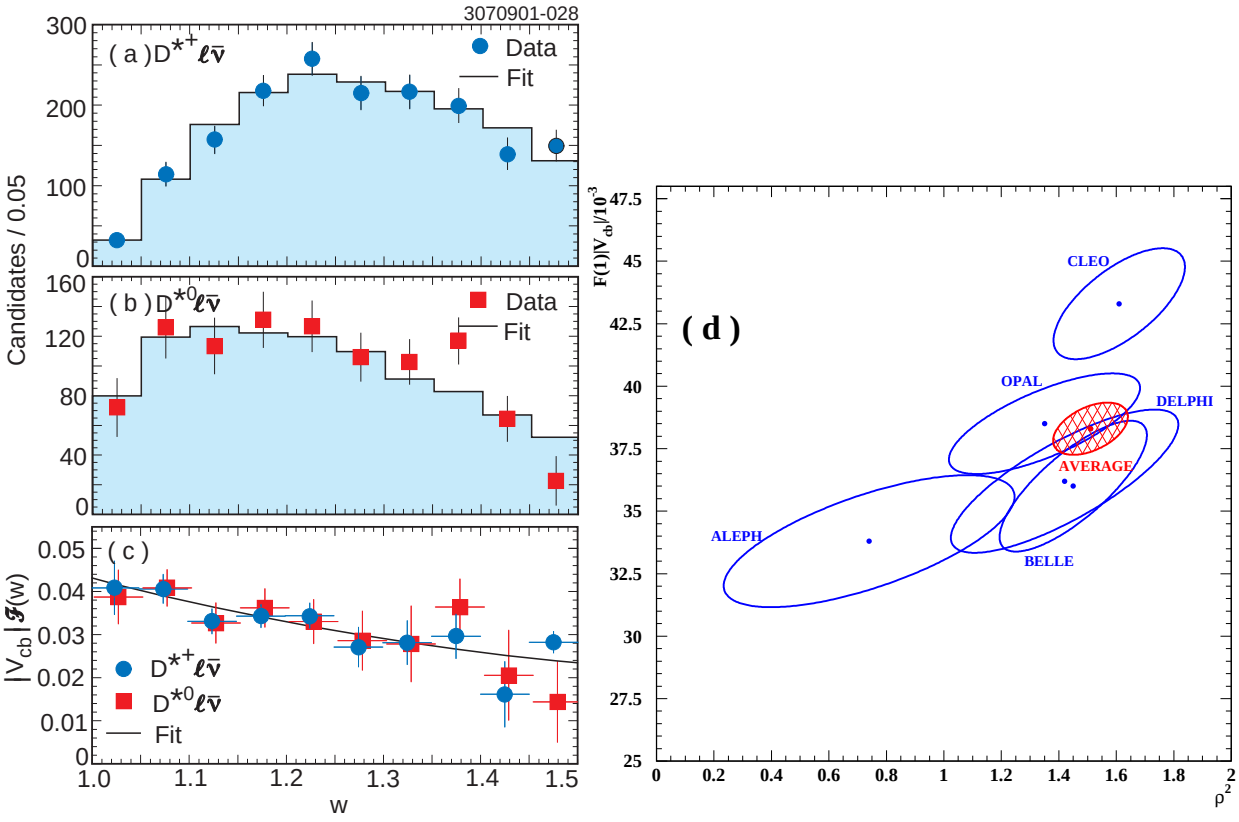

Fig. 3. V_{cb} *in exclusive decays. Signal yield for* $D^{*+}\ell\overline{\nu}$ *(a)* $D^{*0}\ell\overline{\nu}$ *(b) unfolded spectrum (c), comparison of fit results from different experiments (d).*

V_{ub} **from inclusive decays** The lepton endpoint region provides clear evidence for the existence of $b\to u$ transitions. CLEO has published an updated measurement[13] of V_{ub} with the inclusive branching fraction. $\mathcal{B}(B\to X_u\ell\nu)$, based on the CLEO II+II.5 data sets. The measurement of $\mathcal{B}(B\to X_u\ell\nu)$ depends on the successful removal of the dominating background due to b $\to$ charm transitions. This can be achieved by exploiting the larger kinematic range of $b\to u$ transitions, which restricts the accessible $b\to u$ lepton spectrum to the endpoint region.

The total uncertainty on V_{ub} depends on the lepton momentum range chosen. At low lepton momenta the huge background from $b\to c$ transitions constitutes a large un-

certainty. We chose the region of $p_\ell = 2.2 - 2.6\,GeV$ for our central value, which approximately minimizes our total uncertainty. We obtain an inclusive branching fraction $\mathcal{B}(B{\to}X_u\ell\nu)$ of $(1.77 \pm 0.29 \pm 0.38) \times 10^{-3}$, where the first error comes from the branching fraction measurement and the second from the extrapolation of the full momentum spectrum. This measurement translates into a value

$$\mathrm{V_{ub}} = (4.08 \pm 0.34 \pm 0.44 \pm 0.16 \pm 0.24) \times 10^{-3},$$

where the first two errors come from the branching fraction and the third and fourth are theory contributions.

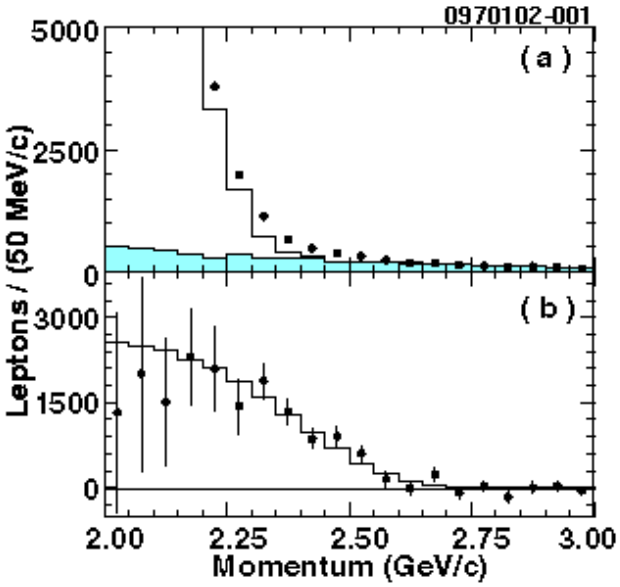

Fig. 4. **(a)** *Lepton spectra for on-resonance data (points) and scaled off-resonance contributions (shaded histo). The open histogram is the total background (off-resonance + background B-decays).*
(b) *Background-subtracted and efficiency corrected lepton spectrum for $B{\to}X_u\ell\nu$ (points). The histogram is the $B{\to}X_u\ell\nu$ prediction based on the $B{\to}X_s\gamma$ spectrum.*

$\mathrm{V_{ub}}$ **from exclusive decays** CLEO has updated the first $B{\to}\pi\ell\nu$ measurement ([14]) with improved statistics and event reconstruction. The larger data sample (CLEO Ii+II.5) allows us to extract signal rates in three independent regions of the momentum transfer q^2. The separation into q^2 bins also permits the test of different form factor models and their q^2 dependence. The preliminary CLEO measurement[15] of the branching fraction $\mathcal{B}(B^0{\to}\pi^-\ell^+\nu) = (1.376 \pm 0.180^{+0.116}_{-0.135} \pm 0.008 \pm 0.102 \pm 0.021) \times 10^{-4}$ is

based on a form factor parameterization[16] consistent with our sub results in the q^2 bins. From $\mathcal{B}$ we derive a preliminary value of $|\mathrm{V_{ub}}| = (3.25 \pm 0.21^{+0.16}_{-0.18}{}^{+0.64}_{-0.56} \pm 0.12 \pm 0.07) \times 10^{-3}$, where the uncertainties are statistical, systematic, and theory uncertainties from the $\pi\ell^+\nu$ form factor, $\rho\ell^+\nu$ form factor and from uncertainties due to other background from B decays. We also obtain branching fractions for $B^0 \to \rho^-\ell\nu$ and $B^+ \to \eta\ell^+\nu$.[15]

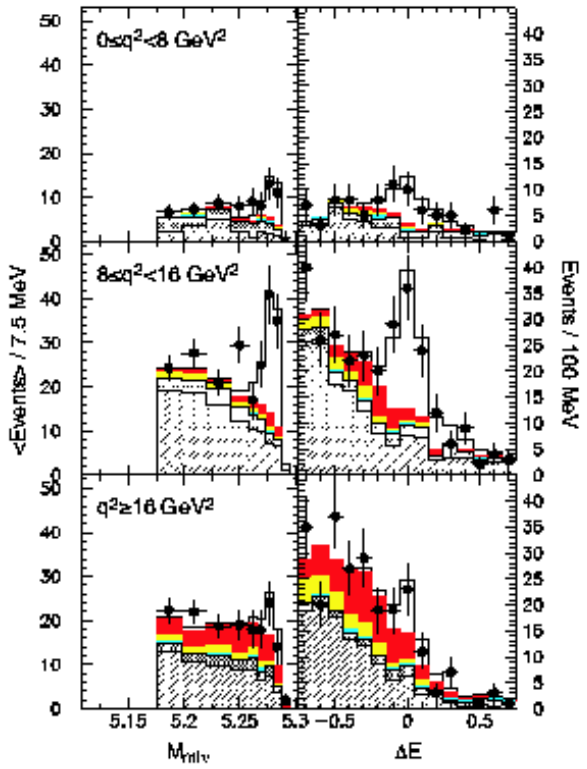

Fig. 5. *Reconstructed B mass ($M_{m\ell\nu}$) and energy difference ΔE in the three q^2 regions for $B \to \pi\ell\nu$ Shown are on-resonance data (points), shaded histogram components are background, open histo is signal.*

The combination of quark mixing matrix results is an on-going project. Common systematic effects and theoretical uncertainties need to be taken into account. The resulting averages have only slightly smaller total errors than individual measurements,[7].[17] The high statistics data samples accumulated by the B-factories in the coming years will probably provide new measurements of $\mathrm{V_{cb}}$ and $\mathrm{V_{ub}}$ using fully reconstructed $\Upsilon(4S)$ events.[18]

3 Rare and Hadronic B decays

The simplest B decay is the external spectator diagram given in Fig. 6. In hadronic decays the internal spectator diagram is also possible. In the case of $B^{\pm}$ decays this diagram can interfere with the external spectator while it leads to unique final states in neutral B meson decays.

Phenomenological parameters a_1 and a_2 are introduced to absorb non-perturbative contributions to the external and internal spectator amplitudes, respectively. While theoretical results show that a_1 is process-independent,[19] and one value is sufficient to describe all decays, the process-independence of a_2 has no theoretical basis and experimental measurements are needed here.

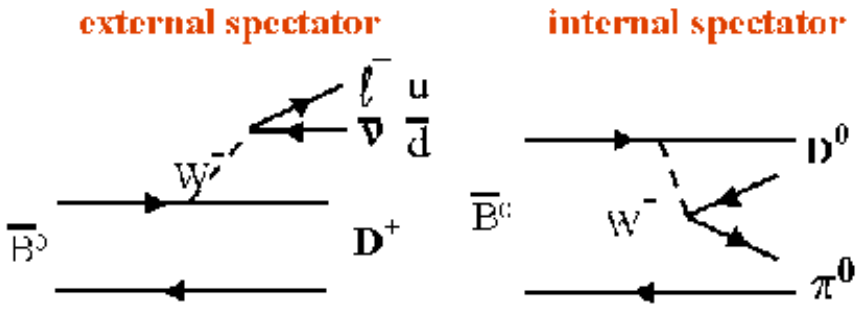

Fig. 6. *Example decay diagrams of B meson decays: external spectator, internal spectator diagram.*

CLEO has dominated for a long time the measurement of exclusive B decays as well as other areas of B physics. Comparing the CLEO measurements of hadronic B decays with the new results from Belle and Babar, we find excellent* agreement.[20]

It is thus no surprise that measurements of exclusive hadronic B decays have reached sufficient precision to challenge our understanding of the dynamics in B decays. In analogy to semileptonic decays, two-body hadronic decay amplitudes might be expressed as the product of two independent hadronic currents, one describing the formation of a charm meson and the other the transition of the virtual W^- into hadron(s). Considering the relatively large energy release in B meson decays, the $u\bar{d}$ pair, which is produced in a color singlet, travels fast enough to leave the interaction region without influencing the second hadron formed from the c quark and the spectator anti-quark.

*The branching fraction for $B^- \to \phi K-$ might need further study. The Belle and Babar measurements in the PDG 2002 edition are not quite in agreement while the CLEO measurement is consistent with both Belle and Babar.

The assumption that the amplitude can be expressed as the product of two hadronic currents is called "factorization".[5] This argument favors the external spectator diagrams.

The internal spectator decay mode is suppressed compared to external spectator processes, since the color of the quark-pair originating from the W decay must match the color of the other quark pair. In the decays of charm mesons, the effect of color-suppression is present but final state interactions, or non-factorizable contributions obscure its observation. The factorization is not as clear as in the B meson system, due to the smaller momentum transfer in charm decays. The concept of color suppression is, however, much clearer in the B meson system.

Until recently the $B\to$ charmonium + X transitions were the only identified color-suppressed B decays. CLEO[21] and Belle[22] have recently observed the color suppressed decays $\overline{\mathrm{B}}^0\to D^{(*)0}\pi^0$.† The CLEO results are $\mathcal{B}(\overline{\mathrm{B}}^0 \to \mathrm{D}^0\pi^0) = (2.74^{+0.36}_{-0.32} \pm 0.55)\times10^{-4}$, and $\mathcal{B}(\overline{\mathrm{B}}^0 \to \mathrm{D}^{*0}\pi^0) = (2.20^{+0.59}_{-0.52} \pm 0.79)\times10^{-4}$.

The signal yield is obtained from an unbinned, extended maximum likelihood fit. The free parameters of the fit are the number of signal events, background from B decays, and from continuum $\mathrm{e^+e^-}$ annihilation. Four variables are used as input to the maximum likelihood fit: the beam-constrained mass M_B, the energy difference ΔE, the Fisher Discriminant $\mathcal{F}_D$, which is a combination of event shape variables, and the cosine of the decay angle of the B $\cos\theta_{B-Hel.}$, defined as the angle between the D momentum and the B flight direction calculated in the B rest frame. The likelihood of the B candidate is the sum of probabilities for the signal and two background hypotheses with relative weights maximizing the likelihood. Fig. 7 demonstrates the significance of our result. Comparing our result to two-body B decays to charmonium the process dependence of the phenomenological parameter a_2 is favored.[24]

The observation of $\overline{\mathrm{B}}^0 \to \mathrm{D}^0\pi^0$ completes the measurement of $\mathrm{D}\pi$ final states and allows us perform an isospin analysis and to extract the strong phase difference, δ_I, between isospin 1/2 and 3/2 amplitudes.[3,25] CLEO has improved its previous measurements of the color-favored $B\to D\pi$ decays[26]

$$\mathcal{B}(B^-\to D^0\pi^-) = (49.7 \pm 1.2 \pm 2.9 \pm 2.2) * 10^{-4},$$

$$\mathcal{B}(\overline{\mathrm{B}}^0\to D^+\pi^-) = (26.8 \pm 1.2 \pm 2.4 \pm 1.2) * 10^{-4},$$

where the errors are statistical, systematic and the error from the uncertainty on the $\Upsilon(4S)$ branching fraction.[26] Because the error distribution of the phase δ_I is highly

†Babar has also preliminary results for $\overline{\mathrm{B}}^0 \to \mathrm{D}^0\pi^0$.[23]

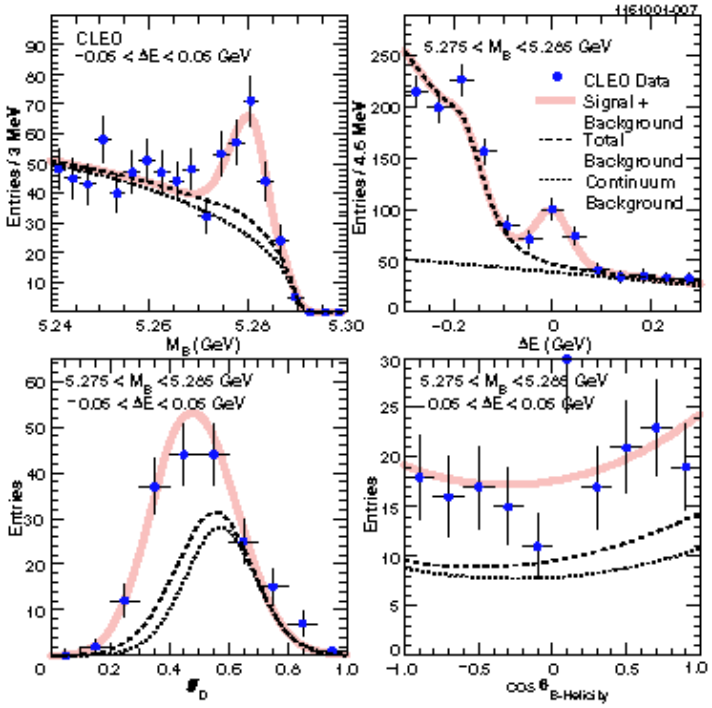

Fig. 7. $\overline{\mathrm{B}}^0 \to D^0\pi^0$. *The results of the unbinned, extended maximum likelihood fit are shown as the full line. The dotted line represents the fitted continuum and the dashed line is the fit result for the sum of* $B\overline{B}$ *and continuum background. To enhance the signal for display purposes, the fit results are projected into the* M_B-ΔE *signal region.*

asymmetric and non-Gaussian, we quote the cosine of the angle. We obtain $\cos\delta_I = 0.863^{+0.024+0.036+0.038}_{-0.023-0.035-0.030}$ based on the CLEO color-favored (Fig. 8) and Belle's+CLEO's color-suppressed results. The significance for the non-zero phase δ_I is 2.3σ which suggests final state interactions. The fourth error on $\cos\delta_I$ is the uncertainty of the $\Upsilon(4S)$ branching fraction. The uncertainty on this basic quantity affects significantly the extraction of final state phases. The same is true for the extraction of (weak) phases in $B \to \pi\pi$ once the signal yields are measured with high enough precision. This has consequences for the unitarity triangle since the extraction of the angle γ relies on the extraction of phases from the $B \to \pi\pi$ branching fractions. The occurrence of final state interactions might also obscure the extraction of γ.[27]

$B \to K\pi\pi$ CLEO measurement of charm-less hadronic two-body decays have received considerable attention because of their importance for unitarity triangle measurements. A natural extension of these measurements are three-body modes. These modes might

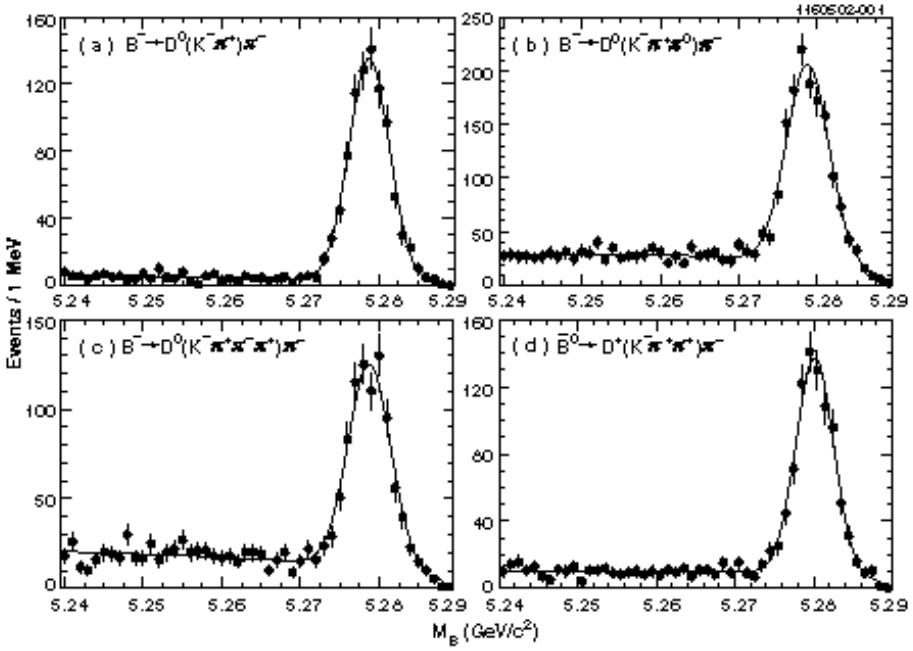

Fig. 8. *The M_B distributions for the $B \to D\pi$ candidates.*

reveal two-body channels with intermediate vector resonances which provide complementary information for the unitarity triangle measurements.

CLEO analyzed $K^0_s h^+ pi^-$, $K^+ h^- \pi^0$ and $K^0_s h^+ \pi^0$, where $h_\pm$ denotes a charged pion or kaon.[28] Obvious contributions from B decays into charm are removed from our sample by cuts on the invariant masses, namely, $B \to D\pi$, $D \to K\pi$ in addition to $B \to J/\Psi K^0$, $J/\Psi \to \mu^+\mu^-$, where the muons are misidentified as pions. Signal yields are extracted from unbinned maximum likelihood fits with several Dalitz contributions. Interference between these amplitudes is neglected and taken into account as a systematic uncertainty.

We derive limits between 19 and 66 $\times 10^{-6}$ for five decay modes and observe $B \to K^0\pi^+\pi^-$ with a branching fraction of $\mathcal{B} = (50^{+10}_{-9}(stat) \pm 7(syst)) \times 10^{-6}$. We perform Dalitz plot fits to search for a substructure and find a contribution from $B \to K^{*+}(892)\pi^-$. Since this mode contributes also to $B \to K^+\pi^0\pi^-$ via $K^{*+}(892) \to K^+\pi^0$, we fit these two modes simultaneously. The branching fraction is $\mathcal{B}(B \to K^{*+}(892)\pi^-)$ = $(16^{+6}_{-5} \pm 2) \times 10^{-6}$ and the signal is 4.6 σ significant. Our results are shown in Fig. 9.

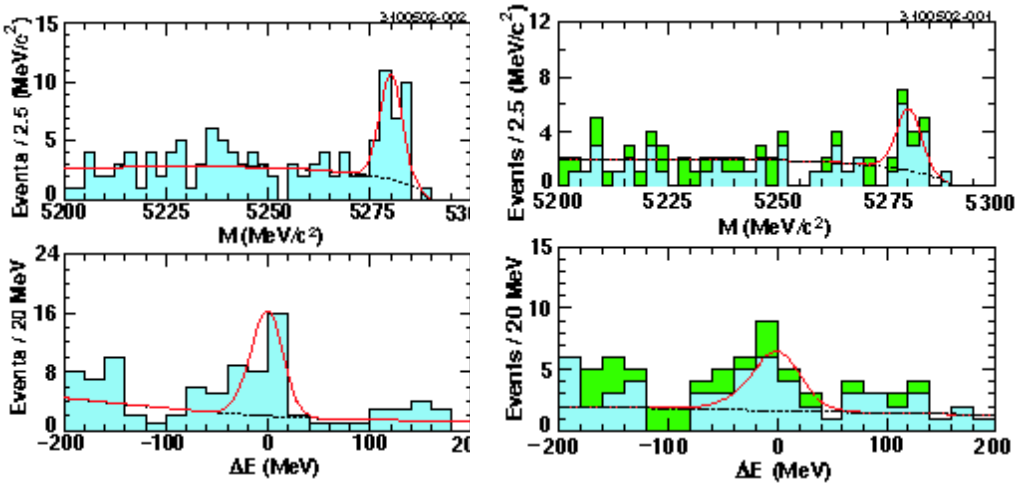

Fig. 9. *M and ΔE projections for $B\to K^0\pi^+\pi^-$ (left), and $B\to K^{*+}(892)\pi^-$ (right). The latter includes the two $K^{*+}(892)$ submodes, $K^{*+}(892)\to K^0\pi^+$ (light shade) and $K^{*+}(892)\to K^+\pi^0$ (dark shade). The background has been suppressed in the plot by a cut on event probabilities. Fit results for background (dashed line) and signal+background (full line) are also shown.*

Baryonic B decays Decays of B hadrons into final states containing a baryon-antibaryon pair have been known for some time. The inclusive rate of $B\to\Lambda_c^+ + X$ is about 5%, much larger than the sum of exclusive decay modes. This suggest significant contributions from final states containing a baryon-antibaryon pair and multiple pions. We report new measurements[29] of exclusive decays of B mesons into final states of the type $\Lambda_c^+\overline{p}n(\pi)$, where $n = 0, 1, 2, 3$. We find signals in modes with 1, 2 and 3 charged pions and we derive an upper limit for the two-body decay into $\Lambda_c^+\overline{p}$. Our measurements are in good agreement with our old results.[30] We obtain the branching fractions given in Table 2. The beam-constrained mass of these decay modes is given in Fig. 10, left side. We derive only a limit on the simplest two-body decay mode $B\to\Lambda_c^+\overline{p}$. Our limit is in agreement with the recent observation of this mode by Belle.[31]

The Λ_c^+ and one of the pions might come from higher resonances. We have searched for a substructure in the various Dalitz decay plots. Fig. 10, right side, shows the distribution of the $\Lambda_c^+\pi - \Lambda_c^+$ mass difference in the vicinity of the Σ_c resonances. Utilizing CLEO's precise mass and width measurements of these resonances,[32] we are able to estimate the significance of our signals and derive branching fractions for several modes (see Table 2).

Again, we have **not** observed true two-body decay modes (of the form $B\to\Sigma_c\overline{p}$).

Mode	$\mathcal{B}$ (10^{-4})	Previous Result (10^{-4})[30]
$\Lambda_c^+\overline{p}$	< 0.9	< 2.1
$\Lambda_c^+\overline{p}\pi^-$	$2.4 \pm 0.6^{+0.19}_{-0.17} \pm 0.6$	6 ± 3
$\Sigma_c^0\overline{p}$	< 0.8	
$\Lambda_c^+\overline{p}\pi^-\pi^+$	$16.7 \pm 1.9^{+1.9}_{-1.6} \pm 4.3$	13 ± 6
$\Sigma_c^0\overline{p}\pi^+$	$2.2 \pm 0.6 \pm 0.4 \pm 0.6$	
$\Sigma_c^{++}\overline{p}\pi^-$	$3.7 \pm 0.8 \pm 0.7 \pm 1.0$	
$\Lambda_{c1}^+\overline{p}$	< 1.1	
$\Lambda_c^+\overline{p}\pi^-\pi^+\pi^-$	$22.5 \pm 2.5^{+2.4}_{-1.9} \pm 5.8$	< 15
$\Sigma_c^0\overline{p}\pi^+\pi^-$	$4.4 \pm 1.2 \pm 0.5 \pm 1.1$	
$\Sigma_c^{++}\overline{p}\pi^-\pi^-$	$2.8 \pm 0.9 \pm 0.5 \pm 0.7$	
$\Lambda_{c1}^+\overline{p}\pi^-$	< 1.9	
$\Lambda_c^+\overline{p}\pi^-\pi^0$	$18.1 \pm 2.9^{+2.2}_{-1.6} \pm 4.7$	< 31
$\Sigma_c^0\overline{p}\pi^0$	$4.2 \pm 1.3 \pm 0.4 \pm 1.1$	

Table 2. *Branching fractions or 90% C.L. upper limits from CLEO*[29] *compared to our old results.*[30] *Substructure results are given in the indented rows. The second error in the branching fraction is due to all systematic uncertainties except for the uncertainty due to the measurement of the* $\Lambda_c^+ \to pK^-\pi^+$ *branching fraction, which is kept separate and appears as a third uncertainty.*

Our newly observed three-body decay modes $\overline{\mathrm{B}}^0 \to \Sigma_c^{++}\overline{p}\pi^-$, $\overline{\mathrm{B}}^0 \to \Sigma_c^0\overline{p}\pi^+$, $\overline{\mathrm{B}}^0 \to \Sigma_c^0\overline{p}\pi^0$ have essentially identical phase space, but only the Σ_c^{++} decay can proceed via both external and internal spectator diagrams, whereas the Σ_c^0 decay can only proceed via an internal spectator diagram. We find the the rate of all three decay modes to be of the same order. This implies that the external W decay diagram does not dominate over the internal spectator, although naively we would expect the latter to be color-suppressed.

The large discrepancy compared to color-suppressed B decays into mesons might be explained by the smaller momentum transfer in baryonic B decays due to the larger mass of the baryon-antibaryon system. A different explanation is given in.[33]

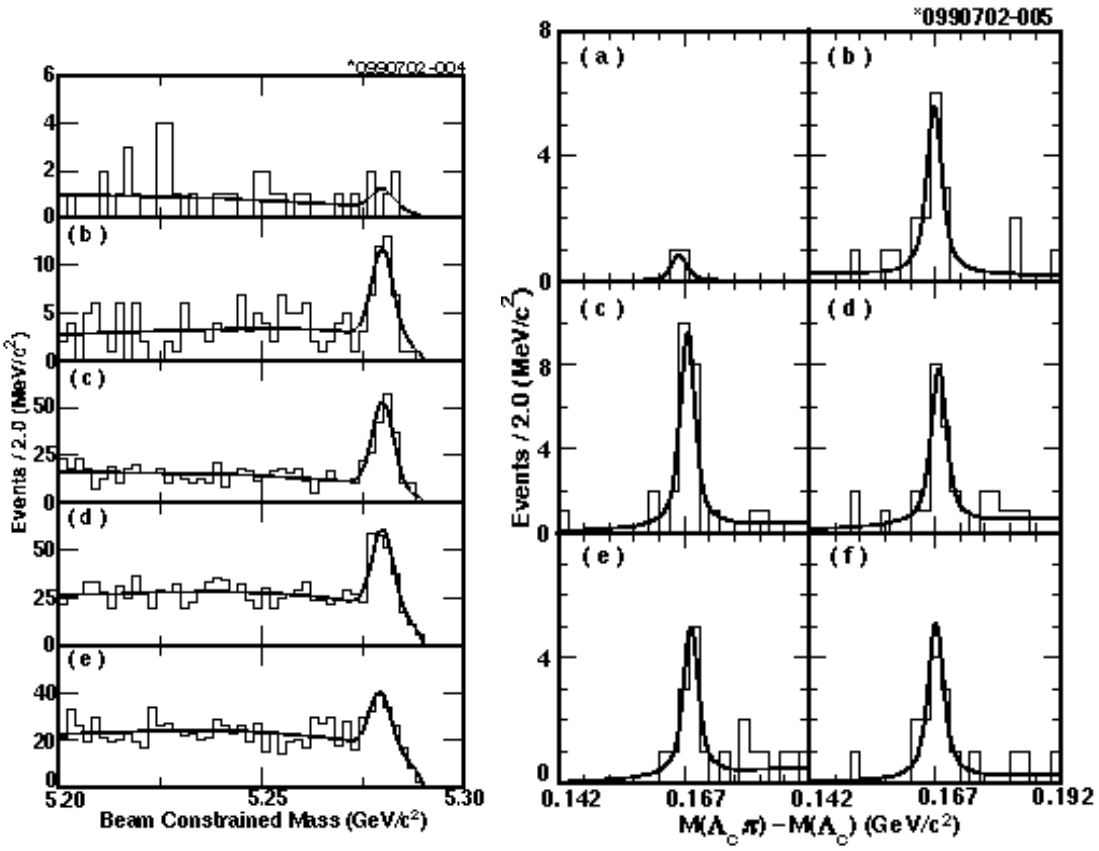

Fig. 10. *left side: Beam constrained mass distributions for a)* $\Lambda_c^+\overline{p}$*, b)* $\Lambda_c^+\overline{p}\pi^-$*, c)* $\Lambda_c^+\overline{p}\pi^-\pi^+$*, d)* $\Lambda_c^+\overline{p}\pi^-\pi^+\pi^-$*, e)* $\Lambda_c^+\overline{p}\pi^-\pi^0$

right side: $M(\Lambda_c^+\pi)-M(\Lambda_c^+)$ *mass differences. a)* $\Lambda_c^+\overline{p}\pi^-$*, b)* $\Lambda_c^+\pi^-$ *within* $\Lambda_c^+\overline{p}\pi^-\pi^+$*, c)* $\Lambda_c^+\pi^+$ *within* $\Lambda_c^+\overline{p}\pi^-\pi^+$*, d)* $\Lambda_c^+\pi^-$ *within* $\Lambda_c^+\overline{p}\pi^-\pi^+\pi^-$ *both combinations, e)* $\Lambda_c^+\pi^+$ *within* $\Lambda_c^+\overline{p}\pi^-\pi^+\pi^-$*, f)* $\Lambda_c^+\pi^-$ *within* $\Lambda_c^+\overline{p}\pi^-\pi^0$.

4 $\Upsilon(3S)$ Spectroscopy

The spectroscopy of bound $b\overline{b}$ states is an excellent testing ground for lattice QCD.[34] The spin-triplet S-wave states $\Upsilon(nS)$ with $J^{PC} = 1^{--}$ are produced in e^+e^- annihilation. These states can decay radiatively with an electric dipole transition (E1) to the spin-triplet P-wave levels, $\chi_b(nP_J)$. Subsequent decays can either return to a lower $\Upsilon(nS)$ state, to the spin-singlet S-wave states $\eta_b(nS)$ or the $\Upsilon(nD)$ states. Neither of the $\eta_b(nS)$ or the $\Upsilon(nD)$ state had been observed by CLEO-II, ARGUS or CUSP. CLEO-III has accumulated new data sets on the $\Upsilon(1S)$, $\Upsilon(2S)$ and $\Upsilon(3S)$, that are comparable in size or larger than the existing world data sets. The first set to become available for data analysis were 4.73 Million $\Upsilon(3S)$ decays collected with the CLEO-III detector. The CLEO-III sample constitutes roughly a ten-fold increase in $\Upsilon(3S)$ statistics compared to the CLEO-II data set.[35]

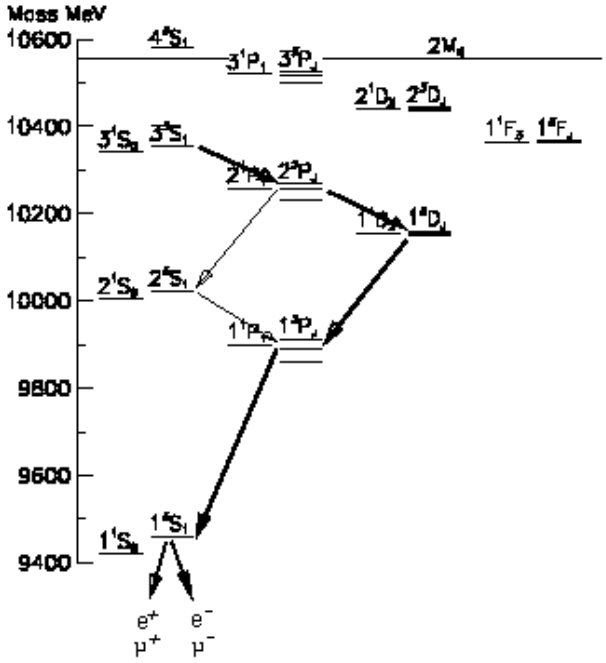

Fig. 11. *Mass spectrum of bound $b\overline{b}$ states.*

Search for the $\eta_b(1S)$. The $\eta_b(1S)$ is the ground state of the $b\overline{b}$ system. To reach the $\eta_b(1S)$, it is necessary to detect either favored magnetic dipole transitions (M1) with very small photon energies or hindered M1 transitions with changes in the prin-

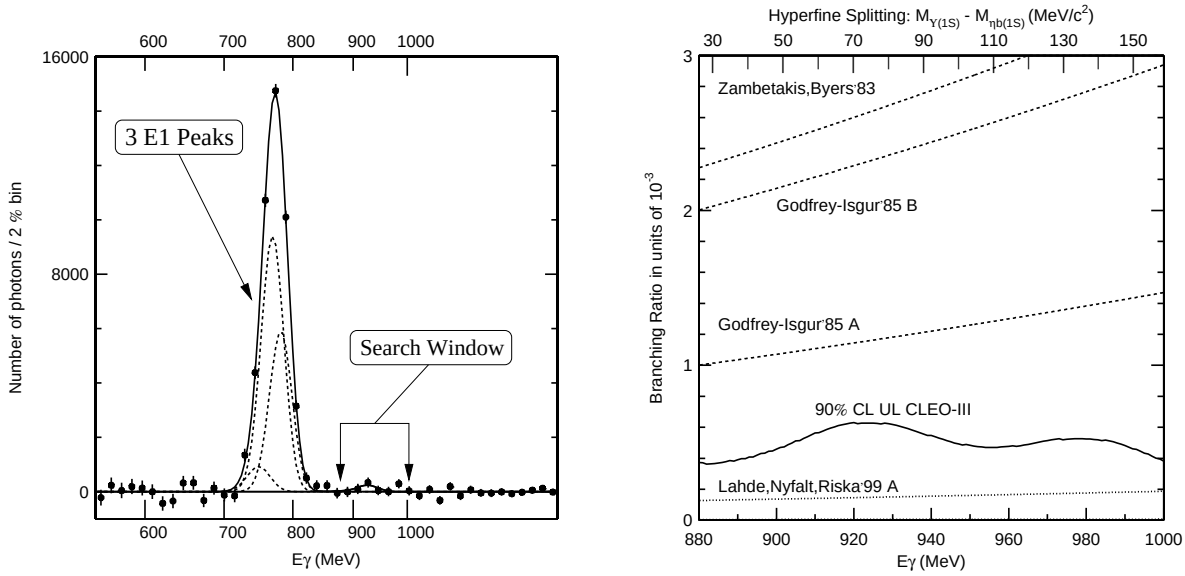

Fig. 12. **(left)** *Background subtracted photon spectrum in the $\chi_b(2P_J)\to\gamma\Upsilon(1S)$ region ($\sim$780 MeV) and the search window. The background was subtracted with a polynomial fit plus a Gaussian for the E1 peak.* **(right)** *Preliminary upper limits on $\mathcal{B}(\Upsilon(3S)\to\eta_b(1S)\gamma)$ with 90% confidence level. Predictions are taken from.*[36]

cipal quantum number. Since there are abundant exclusive decay modes of the η_b[‡] an inclusive search strategy is the most promising approach. Since the M1 transition $\Upsilon(1S)\to\eta_b(1S)\gamma$ is suffering from a small phase space and a huge low-energy photon background, the hindered M1 transition is a promising decay mode.

We analyze the inclusive photon spectrum of well-contained hadronic events on the $\Upsilon(3S)$ resonance. The range of theoretical predictions of the $\eta_b(1S)$-mass define a search window that corresponds to photon energies between 880 to 1000 MeV. In this energy range the largest background arises from photons from π^0 decay. We reject photons that can be paired with another photon to form a π^0 candidate. The sensitivity of our search can be investigated with a peak in the photon energy spectrum due to $\chi_b(2P_J)\to\gamma\Upsilon(1S)$ transitions. This peak is at around 780 MeV – well below our search window. Figure 12 shows the background-subtracted photon spectrum. The peak for $\chi_b(2P_J)\to\gamma\Upsilon(1S)$ demonstrates our good sensitivity to photons from radiative transi-

[‡]So far only one search for the $\eta_b(1S)$ via exclusive decay modes has been proposed,[37] utilizing the expected branching fraction $\eta_b(1S)\to J/\Psi J/\Psi$ of order $7\times10^{-5}-7\times10^{-3}$. This strategy might be applicable at the Tevatron.

tions. We perform a series of fits with a Gaussian signal shape assuming several peak energies, obtaining a maximum signal yield of 698 ± 463 which is only 1.5σ significant. Since we do not find evidence for a signal, we set upper limits on $\mathcal{B}(\Upsilon(1S) \to \eta_b(1S)\gamma)$. The preliminary $\mathcal{B}$-limits as function of the photon energy E_γ are shown in Fig. 12, right side. We exclude most model predictions[36] with a C.L. of 90% or better.[38]

Two-photon cascades of the $\Upsilon(3S)$. CLEO has updated its analysis of the $\chi_b(2P_J)$ states in an analysis of the cascade decay $\Upsilon(3S) \to \chi_b(2P_J)\gamma$; $\chi_b(2P_J) \to \gamma\Upsilon(nS)$; $\Upsilon(nS) \to \ell^+\ell^-$, with n=1,2. We obtain new, preliminary mass measurements[39]

$$m(\chi_b(2P_2)) = (10268.75 \pm 0.30(stat.) \pm 0.58(syst.))MeV$$

$$m(\chi_b(2P_1)) = (10255.64 \pm 0.17(stat.) \pm 0.60(syst.))MeV$$

and also updated our previous branching fraction results. In addition these measurements are an important cross-check of multi-photon cascades, the four-photon cascades probably being the most interesting.

Discovery of the $\Upsilon(1D)$. Recent interest in quarkonium spectroscopy arises from the possibility that our measurements will aid theorists in understanding heavy quarkonium from first principles QCD, given that there is a wide variety of the spin-dependent splittings predicted by several calculations. The discovery of new $b\overline{b}$ states would pose an important test. One proposed search strategy[40] for the D-wave state is via four-photon cascades from the $\Upsilon(3S)$ down to the $\Upsilon(1S)$. The signature of four-photon cascades can stem from several different sources.

- Photon cascade via the $\Upsilon(2S)$:
  $\Upsilon(3S) \to \chi_b(2P_J)(+\gamma) \to \Upsilon(2S)(+\gamma) \to \chi_b(1P_J)(+\gamma) \to \Upsilon(1S)(+\gamma)$
- Hadronic transition
  $\Upsilon(3S) \to \pi^0\pi^0\Upsilon(1S)$
- Photon cascade via the $\Upsilon(1D)$:
  $\Upsilon(3S) \to \chi_b(2P_J)(+\gamma) \to \Upsilon(1D)(+\gamma) \to \chi_b(1P_J)(+\gamma) \to \Upsilon(1S)(+\gamma)$

The latter source is the signal we are looking for. CLEO has made the first observation of the $\Upsilon(1D)$ with these four-photon cascades.[41] Requiring that the endpoint of the photon cascade, the $\Upsilon(1S)$, decays into a pair of leptons, we have a clean signature of $4\gamma\ell^+\ell^-$. Cascades compatible with hadronic transitions $\Upsilon(3S) \to \pi^0\pi^0\Upsilon(1S)$ or

four-photon cascades via the $\Upsilon(2S)$ are vetoed. Due to an unfortunate combination of spin constraints, the latter veto also removes the largest part of the expected $\Upsilon(1D_{J=3})$ signal for most of the mass range, leaving us sensitive to two out of three $\Upsilon(1D)$ states.

The kinematics of the signal cascade can easily be reconstructed once the photons have been assigned to the correct part of the decay chain. Two of the four photon energies in the cascade are known, namely $\Upsilon(3S)\to\chi_b(2P_J)+\gamma$ and $\chi_b(1P_J)\to\Upsilon(1S)+\gamma$. The other two energies depend on the mass of the $\Upsilon(1D)$. Uncertainties in the energy measurements increase the difficulty of finding the correct assignment. For each possible assignment of the four photons to the cascade we define a chi-square

$$\chi^2_{1D,J_2P,J_1P} = \sum_{j=1}^{4} \left(\frac{E_{\gamma j} - E^{expected}_{\gamma j}(M_{\Upsilon(1D)})}{\sigma_{E_{\gamma j}}} \right)^2 ,$$

where $E_{\gamma j}$ are the measured photon energies and $E^{expected}_{\gamma j}$ are the expected photon energies from the masses of the $b\overline{b}$ states and the measured photon directions in the cascade. The χ^2_{1D,J_2P,J_1P} depends on the assumed $\Upsilon(1D)$ mass and on the choice of intermediate J_{2P} and J_{1P} states. We assign to each event an $\Upsilon(1D)$ candidate mass, $m(1D)$, which is the mass that minimizes χ^2_{1D,J_2P,J_1P}, trying all possible photon and spin combinations.

Distributions of the most likely mass assignment $m(1D)$ is shown in Fig. 13, left side. From our Monte Carlo simulations we expect to see signal mass peaks with smaller satellite peaks as shown in Fig. 13, right side.

We fitted the data to a one-peak and two-peak hypothesis, assuming the background to be flat. The assumption that there is no mass peak around 10160 MeV produces low confidence level (0.04%) and can be ruled out at the 9.7 sigma level. The results of the fits are displayed in Fig. 14. The two-peak fit gives the best confidence level (58%). From the change of likelihood between the 2-peak and 0-peak hypothesis we derive a significance of the peak around 10160 MeV of 6.8 standard deviations and the significance of the second peak is about 3 sigma. We therefore claim to see at least one state from the $\Upsilon(1D)$ spin-triplet with sufficient significance. The spin assignment of the state around 10160 MeV is either J=1 or J=2 since J=3 is ruled out due to our low sensitivity for that state. Since the J=2 state is predicted to be produced with 6 times larger rate than the J=1 state, we conclude that the J=2 state is the most likely spin assignment with a mass of $m(\Upsilon(1D_2) = (10161.2 \pm 0.7\,stat. \pm 1.0\,syst.)$ MeV (preliminary). The inclusively measured product branching fraction $\mathcal{B}(\Upsilon(3S)\to\chi_b(2P_J))\times \mathcal{B}(\chi_b(2P_J)\to\Upsilon(1D))\times\mathcal{B}(\Upsilon(1D)\to\chi_b(1P_J))\times\mathcal{B}(\chi_b(1P_J)\to\Upsilon(1S))\times\mathcal{B}(\Upsilon(1S)\to\ell^+\ell^-)$,

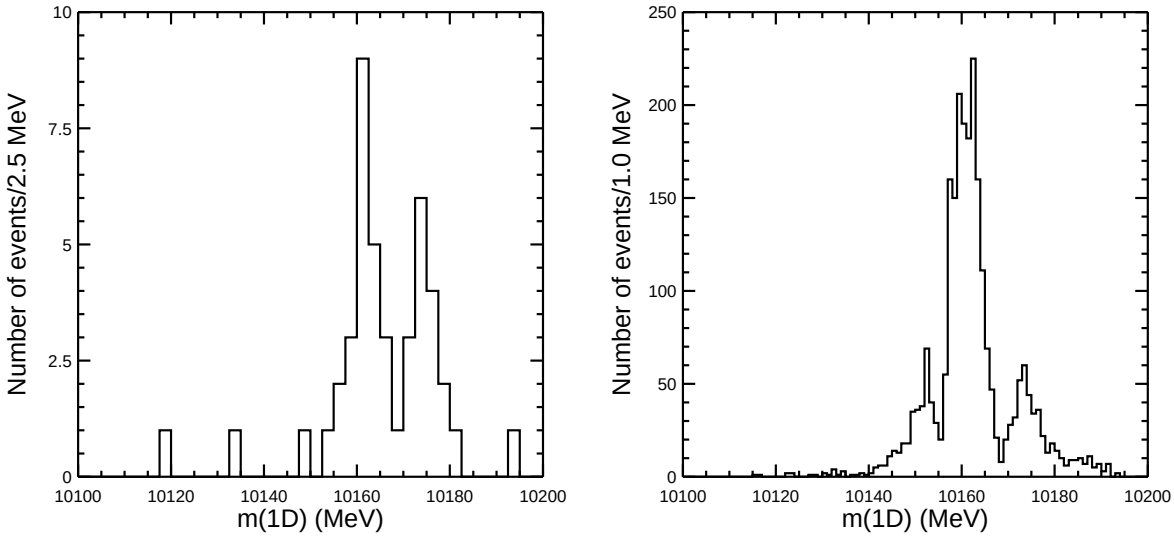

Fig. 13. **left side:** *Distributions of the most likely mass assignment* $m(1D)$. **right side:** *Monte Carlo simulation of the reconstructed mass m(1D) for an* $\Upsilon(1D)$ *state of M=10160 MeV.*

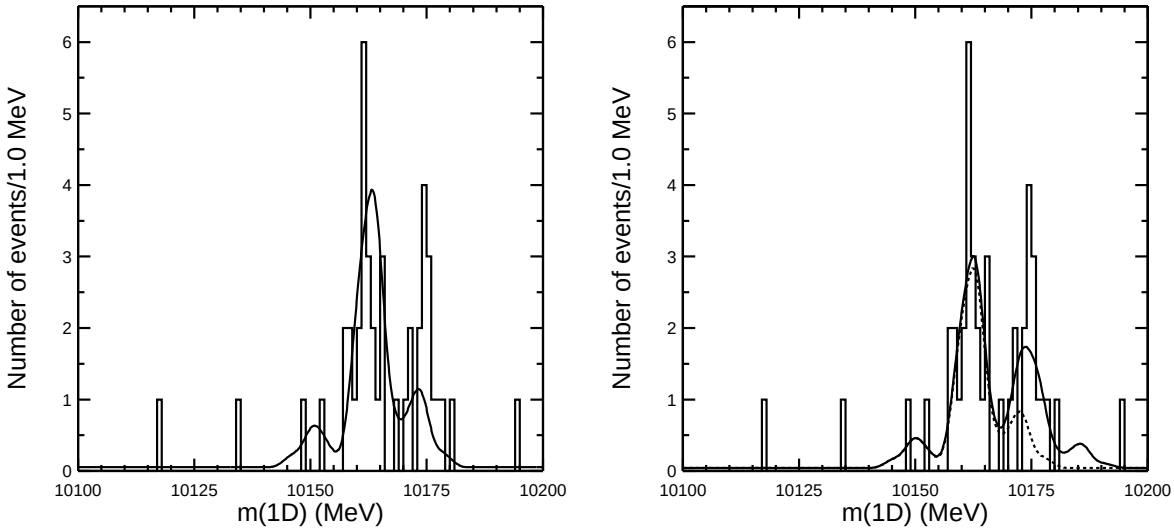

Fig. 14. *Fit of the Monte Carlo signal shape plus a flat background to the data.* **Left side:** *1-peak hypothesis*, **right side:** *2-peak hypothesis*

averaged over the e^+e^- and $\mu^+\mu^-$ modes is $(3.3 \pm 0.6 \pm 0.5) \times 10^{-5}$ (preliminary). This is in good agreement with the theoretical predictions by Godfrey and Rosner.[40]

5 CLEO-c

The CLEO collaboration and CESR plan to operate in the next years at center-of-mass energies in the τ/charm region.[6] This will expand the scope of our on-going charm physics program and will allow precision tests of perturbative and lattice QCD predictions. The results will have an impact on b-quark physics, because heavy flavor physics, and specifically, the extraction of CKM matrix parameters depends on our control over non-perturbative strong interaction effects. An appealing theory for strongly-coupled systems is lattice QCD (LQCD). New LQCD approaches have produced a wide variety of calculations of non-perturbative quantities with accuracies in the 1-20% level for systems containing heavy quark(s). The techniques needed to reduce uncertainties to 1-2% exist, but higher precision requires cross checks for the theory predictions. The probably most important verification of LQCD predictions are charm data that will be collected with CLEO-c. CLEO has the potential to verify LQCD predictions at the 1-2% level. The level of verification will greatly improve the trust of the physics community in LQCD applications.

The list of CLEO-c physics topics is long: charm decay constants f_D and f_{D_s}, absolute charm branching fractions. semi-leptonic decay form factors, direct determination of $\mathrm{V_{cd}}$ and $\mathrm{V_{cs}}$ with 1-2% accuracy, spectroscopy of charmonium states, searches for QCD exotics like hybrids and glueballs, R measurements, rare D decays, D mixing, τ decays.[42,43,6]

These physics topics require an e^+e^- collider operating on the charmonium states J/Ψ Ψ' and $\Psi(3770)$. The $\Psi(3770)$ is the first $c\overline{c}$ resonance above $D\overline{D}$ threshold. The final state is rather limited since the resonance is below threshold for $D\overline{D}\pi$ production. The operation of CLEO-c at this resonance would be analogous to the long and successful running of CLEO on the $\Upsilon(4S)$. Advantages of running there are the excellent signal to background and the probability to tag D-mesons. The tagging is illustrated in Fig. 15. The flavor of the decay $D^0 \to K^-\pi^+$ determines (tags) the flavor of the recoiling D meson. Energy-momentum conservation determines the 4-momentum of the recoiling state.

D-meson tagging makes precise absolute branching fraction measurements possible in addition to un-precedented neutrino reconstruction that is crucial for extracting the

D^+ form factor in the leptonic decay $D^+ \to \mu^+ \nu_\mu$. Another advantage of the $\Psi(3770)$ running is the quantum coherence of the $D\overline{D}$ system which aids D mixing and CP violation studies.

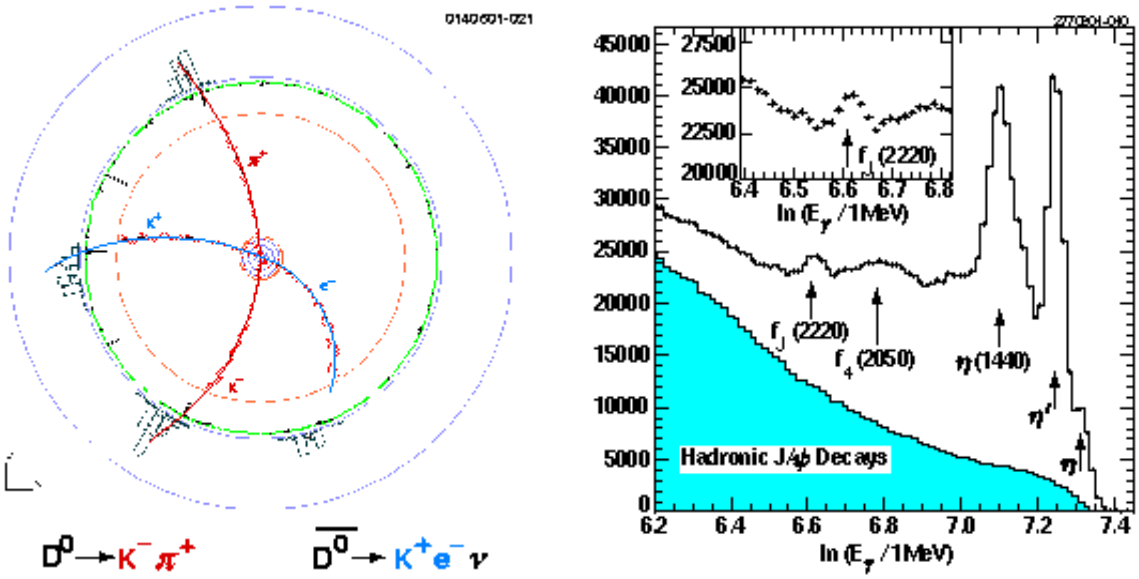

Fig. 15. *Left side: CLEO-c event display of a simulated* $\Psi(3770)$ *decay. Right side: Photon energy spectrum in radiate* J/Ψ *decays as a function of* $\ln(E_\gamma/1\ MeV)$. *The background from hadronic* J/Ψ *decays is included as the shaded area.*

QCD studies with CLEO-c Table 3 shows a summary of the data set size for CLEO-c (projected) and for BES. The CLEO-c data sets will be over an order of magnitude larger. In addition, the CLEO detector is more modern and thus superior to the BES II detector. This will allow us to improve on many BES measurements due to better control over systematics. This can be demonstrated in two examples.

(1) Our hermetic detector with very good track reconstruction efficiency will allow us to perform exact Measurements of R, the ratio of the ISR-corrected hadronic cross section to the first-order QED cross section. The average uncertainty on each energy point of 7% (BES) can be improved with CLEO-c to ∼2% in the range $\sqrt{s} = 3 - 5$ GeV. Electroweak precision fits will benefit from the improved R result.[44]

(2) The energy resolution of our CsI calorimeter is up to 20 times better than BES-II, for example 2% at $E_\gamma = 700$ MeV. This makes measurements of the inclusive photon spectrum in radiative $J/\Psi$and Ψ' decays possible. Radiative J/Ψ decays are an excellent search ground for glue-rich QCD exotics. A CLEO-c photon spectrum from

$J/\Psi \to \gamma + X$ is shown in Fig. 15, right side. The spectrum is based on 7×10^7 simulated J/Ψ decays.

Narrow resonances with branching fractions of order 10^{-4} can easily be identified in radiative decays. E.g. the peak[§] from the $f_J(2220)$ is clearly visible in Fig. 15. Combined with exclusive radiative $\Psi^{(\prime)}$ decays, absolute branching fractions of narrow QCD exotics can be measured. These measurements in addition to a full partial wave analysis of exclusive final states will elucidate the nature of QCD exotics in the mass region below 3 GeV. Our search for glue-rich QCD exotics will be complemented by a search for similar final state in radiative Upsilon decays and an anti-search in two-photon events.

Resonance	CLEO-c	BES-II
J/Ψ	10^9	6×10^7
Ψ'	10^8	4×10^6
$\Psi(3770)$	3×10^7 $D\overline{D}$	–
$E_{CM} = 4140$ MeV	1.5×10^6 $D_s\overline{D}_s$	4×10^5

Table 3. Comparison of projected CLEO-c data samples with BES-II.

6 Summary and Conclusions

Since the whole text is a summary of recent CLEO results, another summary is not in order. Many more interesting CLEO results on B physics will come out in the near future. First CLEO-III results from the $\Upsilon(4S)$ can be expected soon. CLEO has successfully finished operation on the $\Upsilon(1S - 3S)$ resonances and is soon exploring the τ-charm region. First, exploratory runs at lower energies yielded encouraging results. High luminosity runs can be expected as soon as the CESR accelerator upgrade in finished in 2003.[6]

Acknowledgments I would like to thank my CLEO colleagues for giving me the opportunity to present our results. I would also like to gratefully acknowledge the effort of the CESR staff in providing us with excellent luminosity and running conditions. I finally thank the organizers for a wonderful conference experience.

[§]The $f_J(2220)$ is simulated with $\mathcal{B} = 8 \times 10^{-4}$, $M = 2230 MeV$ and $\Gamma = 23 MeV$

References

[1] D. Lange, these proceedings

[2] W. Trischuk, these proceedings

[3] M. Neubert and B. Stech in *Heavy Flavors*, edited by A.J. Buras and M. Lindner (World Scientific, Singapore, 2nd edition 1998).

[4] T. E. Browder, K. Honscheid and D. Pedrini, Ann. Rev. Nucl. Part. Sci. **46**, 395 (1996)

[5] M. Neubert, hep-ph/0006265

[6] R. A. Briere $et\ al.$, CLNS-01-1742 (June 2001)

[7] M. Artuso and E. Barberio, in K. Hagiwara $et\ al.$ (Particle Data Group), Phys. Rev. D **66**, 010001 (2002), [hep-ph/0205163]

[8] D. Cronin-Hennessy $et\ al.$ [CLEO], Phys. Rev. Lett. 87, 251808 (2001)

[9] S. Chen $et\ al.$ [CLEO], Phys. Rev. Lett. 87, 251807 (2001)

[10] A. H. Mahmood $et\ al.$ [CLEO], CLNS 02/1810;
R. Briere $et\ al.$ (CLEO) CLEO-Conf 02-10, hep-ex/0209024

[11] M. Gremm, A. Kapustin, Z. Ligeti and M. B. Wise, Phys. Rev. Lett. **77**, 20 (1996)

[12] R. Briere $et\ al.$ [CLEO], Phys. Rev. Lett. 89, 081803 (2002)

[13] A. Bornheim $et\ al.$ [CLEO], Phys. Rev. Lett. 88, 231803 (2002)

[14] T. E. Browder *et al.* [CLEO], Phys. Rev. D **56**, 11 (1997);
B. H. Behrens *et al.* [CLEO], Phys. Rev. D **61**, 052001 (2000)

[15] N.E. Adam, $et\ al.$ [CLEO], CLEO-Conf 02-09

[16] P. Ball and R. Zwicky, JHEP **0110**, 019 (2001)

[17] M. Battaglia and L. Gibbons, in K. Hagiwara $et\ al.$ (Particle Data Group), Phys. Rev. D **66**, 010001 (2002)

[18] J. Lee and I. Shipsey, in *Proc. of the APS/DPF/DPB Summer Study on the Future of Particle Physics (Snowmass 2001)* ed. N. Graf, hep-ex/0203015.

[19] M. Beneke $et\ al.$, Nucl.Phys. **B591** (2000) 313

[20] K. Hagiwara $et\ al.$ (Particle Data Group), Phys. Rev. D **66**, 010001 (2002)

[21] T. E. Coan $et\ al.$ [CLEO] , Phys. Rev. Lett. 88, 062001 (2002)

[22] K. Abe $et\ al.$ [Belle], Phys. Rev. Lett. 88, 052002 (2002)

[23] B. Aubert $et\ al.$ [BaBar], hep-ex 0207092, subm. to ICHEP 2002

[24] M. Neubert and A. Petrov, Phys. Lett. **B519**, 50 (2001)

[25] J.L. Rosner, Phys. Rev. D **60**, 074029 (1999)

[26] S. Ahmed $et\ al.$ [CLEO], Phys. Rev. D, 66, 031101(R) (2002)

[27] J.P. Silva, A. Soffer, L. Wolfenstein and F. Wu, hep-ph/0209274

[28] E. Eckhardt $et\ al.$ [CLEO], Phys. Rev. Lett. **89**, 251801 (2002)

[29] S.A. Dytman $et\ al.$ [CLEO], Phys. Rev. D 66, 091101(R) (2002)

[30] X. Fu $et\ al.$ [CLEO], Phys. Rev. Lett. **79**, 3125 (1997)

[31] N. Gabychev, H. Kichimi $et\ al.$ [Belle] hep-ex/0212052

[32] M. Artuso ***et al.*** [CLEO], Phys. Rev. D **65**, 071101 (2002)

[33] H. Y. Cheng and K. C. Yang, hep-ph/0210275

[34] P. Lepage, these proceedings

[35] G. Crawford $et\ al.$ [CLEO], Phys. Rev. Lett. **294B** 139 (1992)

[36] S. Godfrey, J. Rosner, Phys. Rev. D **64**, 074011 (2001); erratum ibidum **65** 039901, and references therein.

[37] E. Braaten, S. Fleming and A. K. Leibovich, Phys. Rev. D **63**, 094006 (2001)

[38] A.H. Mahmood $et\ al.$ [CLEO], CLEO-Conf 02-05, hep-ex/0207057

[39] D. Cinabro $et\ al.$ [CLEO], CLEO-Conf 02-07, hep-ex/0207062

[40] S. Godfrey and J.L. Rosner, Phys. Rev. **D64**, 097501 (2001)

[41] S.E. Csorna $et\ al.$ [CLEO], CLEO-Conf 02-06, hep-ex/0207060

[42] I. Shipsey, these proceedings

[43] I. Shipsey, hep-ex/0207091

[44] H. Burkhardt and B. Pietrzyk, Phys. Lett. B **513**, 46 (2001);
J. H. Kuhn and M. Steinhauser, JHEP **0210**, 018 (2002)